Published in final edited form as:
Neuroimage. 2013 April 15; 70: 113–121. doi:10.1016/j.neuroimage.2012.12.040.

Age-Related Differences in Iron Content of Subcortical Nuclei Observed *in vivo*: A Meta-Analysis

Ana Daugherty[1] and **Naftali Raz**[1,2]

[1]Institute of Gerontology and Department of Psychology, Wayne State University, Detroit, MI 48202

Abstract

Accumulation of non-heme iron in the brain has been proposed as a biomarker of the progressive neuroanatomical and cognitive declines in healthy adult aging. Postmortem studies indicate that iron content and lifespan differences therein are regionally specific, with a predilection for the basal ganglia. However, the reported *in vivo* estimates of adult age differences in iron content within subcortical nuclei are highly variable. We present a meta-analysis of 20 *in vivo* magnetic resonance imaging (MRI) studies that estimated iron content in the caudate nucleus, globus pallidus, putamen, red nucleus, and substantia nigra. The results of the analyses support a robust association between advanced age and high iron content in the substantia nigra and striatum, with a smaller effect noted in the globus pallidus. The magnitude of age differences in estimated iron content of the caudate nucleus and putamen partially depended on the method of estimation, but not on the type of design (continuous age vs. extreme age groups).

Keywords

non-heme iron; aging; striatum; red nucleus; substantia nigra

Introduction

Many aspects of the human brain, from molecular processes and gene expression to gross anatomy and systemic physiology, change profoundly with age. However, the magnitude and the pace of change differ among brain regions and vary in their impact on cognitive performance (Raz and Kennedy, 2009). The reasons for the lack of uniformity in the brain aging remain unclear. It may reflect differential sensitivity of brain components to age-related changes in key metabolic and neurochemical processes that affect cellular homeostasis and structural integrity. One such putative marker of age-related cellular vulnerability is iron. Although iron is an essential metabolite that is omnipresent in the neurons and neuritic processes, its excessive accumulation in specific regions of the brain may be a sensitive indicator of increased oxidative stress and thus a marker of age-related vulnerability (Bartzokis, 2011; Mills et al., 2010).

[2]Corresponding author: nraz@wayne.edu; 87 E. Ferry, 226 Knapp Bldg., Detroit, MI, 48202; Phone: (1) 313-664-2617; Fax: (1) 313-664-2667.

Within the brain, iron appears primarily in two forms: intracellular non-heme iron and heme iron that occupies the core of the hemoglobin molecule and thus present in any location where blood flows or accumulates (Tingey, 1938). Whereas heme iron does not appear to play a significant role in oxidative stress and neurodegeneration (Halliwell, 1992; Mills et al., 2010), non-heme iron is an established promoter of reactive oxygen species (ROS) within brain tissue and is thus a potential contributor to cellular deterioration (Mills et al., 2010). As a rule, more than 90% of intracellular non-heme iron is sequestered in ferritin (Gomori, 1936; Hallgren and Sourander, 1958; Lauffer, 1992; Jara et al., 2006), until it is released to meet metabolic demands of neurotransmission, mitochondrial ATP generation, and DNA replication (Chrichton and Ward, 1992; Fisher et al., 2006; Mills et al., 2010). Outside of ferritin, metabolically active (ferric) iron forms a labile pool bound to amino acids (Lauffer, 1992), other metabolites (Cbantchik et al., 2002), and possibly metallochaperones (Mills et al., 2010).

Non-heme iron is unevenly distributed across brain regions and structures, andthe magnitude of age differences in iron contentvaries among the regions. Among the brain components, the basal ganglia have the highest concentrations of iron in early adulthood and show the most substantial age differences (Hallgren and Sourander, 1958; Thomas et al., 1993; Haacke et al., 2005). This pattern of non-heme iron distribution may reflect regional differences in need for iron that is proportional to metabolic demands of neurotransmission (see Mills et al., 2010 for a review). Indeed, dopaminergic transmission that is one of the main modes of neural activity in the iron-rich striatum depends on availability of iron (Zecca et al., 2004).

With iron being a necessary actor in neurotransmission and a potential promoter of apoptosis intracellular stores of ferric iron must be strictly regulated. However, with advanced age, this fine balance gradually changes. As transport and storage mechanisms deteriorate (Singh et al., 2009; Zhang et al., 2009; Bartzokis et al., 2011), metabolically active iron accumulates outside of ferritin, increases oxidative stress, and notably degrades cellular integrity (Mills et al., 2010; Zecca et al., 2004). Although the causal relationship remains unclear, it is known that increased non-heme iron content is associated with atypical dopamine and serotonin metabolism (Berg et al., 2007), mutations in mitochondrial and nuclear DNA (Hamilton et al., 2001), and accelerated apoptosis (Zhang et al., 2009).

Cellular degradation related to iron accumulation might explain the cumulative structural declines that accompany aging and neurodegenerative disease (Harman, 1956). For example, it is plausible that iron plays an important role in Alzheimer's disease (AD), as iron deposits co-localize with tangles (House et al., 2004), plaques (Quintana et al., 2006), and amyloid burden (Rival et al., 2009). According to a recent theory, iron-catalyzed oxidative stress is a primary cause of demyelination in normal aging and accelerated demyelination in AD (Bartzokis, 2011). Elevated iron concentration has been linked to the formation of Lewy bodies (Berg et al., 2007) and decline in the extra-pyramidal motor system (Spatz, 1922).

Iron content is relevant to cognitive performance. In older rodents, iron overload and oxidative stress produce declines in spatial navigation and motor control (Joseph et al., 2005; Maaroufi et al., 2009). In healthy adults, high iron content of the hippocampus contributes to age-related differences in memory (Rodrigue et al., 2012). Greater iron presence in the brain, primarily in the basal ganglia, is associated with general cognitive aptitude in septuagenarians (Penke et al., 2012). However, until recently, information about brain burden of non-heme iron in humans came almost exclusively from post-mortem studies, thereby hampering an understanding of its role in functional and cognitive changes that occur in healthy aging. Thus, the importance of obtaining correct *in vivo* estimates of

brain iron content in healthy adults cannot be overstated, and the recent advent of MRI methods that derive contrast from the presence of iron is encouraging.

A notable feature of iron behavior in the healthy aging brain is significant regional variability in its content (Thomas et al., 1993). In their landmark study, Hallgren and Sourander (1958) quantified regional age-related differences in healthy brains from infancy to the age of 100 years. They found that in younger and middle-aged brains, advanced age was associated with greater iron concentrations in the basal ganglia than in subcortical white matter, but noted that the association between age and iron content was attenuated after middle age (Hallgren and Sourander, 1958). However, the reported estimates of adult lifespan differences in iron content could have been biased by several factors, such as inclusion of pre-adolescent participants and the exponential accumulation of iron in early life (Aquino et al., 2009; Thomas et al., 1993). These factors could have obscured a relatively small, but potentially meaningful, difference across the adult lifespan. The introduction of *in vivo* techniques has offered further insight into the potential role of iron in adult aging.

In principle, MRI is very well suited for *in vivo* assessment of regional iron content in the brain. Paramagnetic materials, such as iron, have very high magnetic susceptibility and, therefore, a short transverse relaxation time (T2) or long relaxation rate (R2). On T2-weighted images, iron-rich regions such as the basal ganglia, red nucleus and substantia nigra appear hypointense. Moreover, low intensity values of these regions are even lower in the brains of older adults (Siemonsen et al., 2008; Thomas et al., 1993). In spite of a strong correlation between T2 and iron content, T2-weighted imaging and T2 relaxometry are not the optimal methods of estimating iron content *in vivo,* as they are sensitive to other factors. For example, decreased water content also results in shortening of T2 and thus may be misinterpreted as increased iron content (Haacke et al., 2005).

To reduce the likelihood of such misinterpretations one can use the field-dependent R2 increase (FDRI) method, which relies on differences in spin-spin relaxation rates obtained from magnets of different field strength. In FDRI, identical sequences with the same acquisition parameters are repeated back-to-back in two different magnets that differ in their field strengths (Bartzokis et al., 2011). In comparison to a single-magnet measure, FDRI yields a more precise estimate of local susceptibility related to iron content. However, the method calls for two different imaging systems. Thus, even with a great similarity of acquisition sequences and a minimal delay between the runs, the FDRI introduces unwanted variability in subject orientation and scanner properties.

The validity of relaxometry as a method for *in vivo* estimation of brain iron content can be improved by using T2*, which is a sum of T2 and T2′ (or R2*, a sum of their reciprocals). T2* and R2* are sensitive to the local field inhomogeneity and are less ambiguously related to the amount of iron in tissue than T2 is (Ordidge et al., 1994; see Haacke et al., 2005 for a review). The main disadvantage of the T2* method is that background field inhomogeneity that is unrelated to iron content may confound the estimates especially in the presence of other para- and diamagnetic elements(see Haacke et al., 2005 for a review). A component of T2*, T2′, is potentially a more precise index of iron content than T2*, but its values are relatively small and difficult to measure with desirable precision.

To rule out the influence of potential confounds, phase information provided by susceptibility-weighted images (SWI; Haacke et al., 2005) has been recently proposed to deliver more precise and specific estimates of iron content than other methods. Regional differences in phase are proportional to iron content, as has been validated by correlation with published postmortem values (Ogg et al., 1999; Haacke et al., 2005). Theoretically,

phase can detect small regional differences in iron content better than T2* estimates and is easier to measure than T2′ (Haacke et al., 2005). Further, phase is directional, and differences in phase direction can distinguish regions of calcification (diamagnetic) from those that contain non-heme iron (paramagnetic) based upon image intensity. However, phase-based estimates of iron content are not entirely problem-free. For example, unlike the T2* and T2′, regional phase values are poorly localized and may be affected by signal from neighboring tissue. New post-acquisition processing methods have been developed to remove non-local effects and to improve regional estimates (Haacke et al., 2010; Langkammer et al., 2012), but at the time of this writing only one study (Bilgic et al., 2011) has used these methods to measure age differences in healthy adults.

Based on a histological study, ferritin and hemosedrin are the only paramagnetic materials of sufficient concentration to affect MR signal from brain tissue (Schenck, 1995). Concentrations of transferrin-bound iron, the labile pool, and soluble iron particles are probably insufficient to cause differences in MR signal (Haacke et al., 2005). Other endogenous paramagnetic materials (i.e., copper and manganese) are also at inadequate concentrations in healthy individuals to affect the signal (Haacke et al., 2005). However, the MRI methods cannot readily distinguish between heme (i.e., cerebral blood volume) and non-heme iron sources, which may correlate highly in subcortical regions (Anderson et al., 2005). Despite their limitations, the various MRI methods have been validated in several phantom studies and in comparison to post-mortem assays (Antonini et al., 1993; Bizzi et al., 1990; Vymazal et al., 1995a; Peran et al., 2009; Pujol et al., 1992; Brass et al., 2006; Thomas et al., 1993; Bartzokis et al., 1994). Like post-mortem observations, MRI studies of adult age differences in iron content have found regional discrepancies, albeit of various magnitudes (Bartzokis et al., 2007; Drayer, 1988; Pfefferbaum et al., 2009; Bartzokis et al., 1997; Pujol et al., 1992; Peran et al., 2009; Cherubini et al., 2009; Xu et al., 2008; Pfefferbaum et al., 2010). Haacke and colleagues (2005) recently commented on the variability among extant MRI studies and post-mortem methods, although the review only listed the results without a specific analysis of regional age differences.

Thus, the goal of this meta-analysis was to evaluate quantitatively the outcomes of studies reviewed in the last narrative review (Haacke et al., 2005) as well as those that appeared after that publication. In the meta-analysis, we focused on the brain regions, age differences in which have been examined in a sufficient number of *in vivo* studies, i.e., globus pallidus (GP), putamen (Pt), caudate nucleus (Cd), red nucleus (RN), and substantia nigra (SN). Finally, our aim was to evaluate two potential sources of discrepancies among the studies in observed age differences: method of iron content estimation and the type of design *vis a vis* age (extreme groups or continuous).

Method

2.1 Sample of Studies

We searched the computerized database PubMed through April 2012. Search terms were “brain iron,” “R2*,” “T2*,” “R2,” “T2,” “R2′,” “T2′,” “FDRI,” “phase,” “susceptibility-weighted imaging (SWI),” “aging,” “age,” “caudate,” “putamen,” “globus pallidus,” “red nucleus,” and “substantia nigra.” Because studies may report age-related differences in regions of interest (ROIs) for the purposes of a control comparison, but not include these as key terms, we performed general searches and reviewed the additional studies manually for reported age differences. Reference lists of review articles, book chapters, and publications meeting the search terms were also reviewed.

2.2 Inclusion Criteria and Study Coding

For initial inclusion, selected studies necessarily reported a relationship between age and *in vivo* brain iron estimation in one of the five ROIs in a healthy sample screened at least for major neurological pathologies, psychiatric conditions, and dementia. Considered studies were in a peer-reviewed publication and available in English. This initial search yielded 49 studies, many of which reported effects within the same sample across multiple ROIs (see Table 1). We contacted authors of studies that met the inclusion criteria but did not report a usable statistic to calculate an effect size, those who estimated brain iron in healthy controls but did not publish age differences, and those who included pre-adolescent children in the sample. Twenty studies that estimated brain iron in healthy control groups were excluded for lack of data. Five studies were excluded because the samples included children under 18 years old, as the relationship of brain iron during childhood development is different from that in adulthood (Aquino et al., 2009). One study was excluded because brain iron was estimated from T1-weighted scans (Vymazal et al., 1995b), which is an incomparable methodology to the others considered. A small-sample study that reported R2′ values (Martin et al., 1998) was excluded because it was the only extant study to use this method to estimate age differences and because the sample was small, and therefore the study could have biased the meta-analysis. Two studies (Bartzokis et al., 2010; 2011) were excluded as each used a sample already reported in the previous study included in the analyses (Bartzokis et al., 2007).

Twenty studies that met the final inclusion criteria and reported complete data were used in the meta-analysis (see Table 1). Besides the inclusion criteria, there were no known systematic differences in samples between the studies included and those excluded. In addition to estimating an average effect size within each ROI, we modeled potential study differences based on MRI estimation method and the treatment of age either as stratified groups or as a continuous distribution. Although we took notice of several other characteristic study variables, such as sample average age and age range, MRI sequences, and magnet strength, we could not analyze these potential moderators due to the limited number of available studies.

2.3 Meta-Analytic Procedures

2.3.1 Computation of effect sizes—Using DSTAT (Johnson, 1993), all relevant study statistics were converted to Pearson correlations (r; see Table 1) and sample-size corrected effect sizes (d). Such correction is of a special concern when studies with small samples are included in the analyses. The computations were based on t-tests, group means and standard deviations, p-values and sample sizes, whole sample correlations (r) or linear regression statistics (R^2). For studies that reported a significant effect without reporting a statistic or p-value, d was conservatively estimated from $p = 0.049$ (i.e., Cherubini et al., 2009). Studies that reported a non-significant effect without a statistic and a sample size smaller than 100 were excluded because a conservative estimate of $r = 0$ may be biased by a small sample (i.e., Antonini et al., 1993 for the Cd and GP). When left and right ROI values were reported, the effects were averaged for a whole ROI estimate prior to calculating d. Only whole GP (i.e., no separation of medial and lateral) and Pt (i.e., no distinction between anterior and posterior) effects were considered. To conform to the relaxation rate (rather than relaxation time) metric, effects from studies estimating iron content from T2 and T2* methods were inverted, so that higher values were associated with larger iron content. When a study reported multiple indices of iron content measured in a single sample (i.e., Pfefferbaum et al., 2010), we selected one measure that was strongest in study design and offered the best statistical power for the moderator analyses. Finally, when whole lifespan samples were used but values were reported by decade, adult age effects were manually estimated (i.e., Aquino et al., 2009).

2.3.2 Statistical methods—To avoid violating the assumption of independent observations, each ROI was analyzed separately. Within each ROI, categorical models for the relationship between age and *in vivo* iron content estimates were tested. The analyses followed the Hedges and Olkin's (1985) approach to meta-analysis with fixed-effects model estimation. This approach allows correction of each effect size for study sample size, as insufficient power is a concern in this sample of studies.

Homogeneity tests for within-class (Q_w) and between-class (Q_b) effect sizes were calculated according to Hedges and Olkin's (1985) procedures. Q_w assessed the homogeneity of effect sizes within each class as a χ^2 distribution with $k - 1$ degrees of freedom, where k is the number of effect sizes within the class; whereas Q_b assessed between classes with $p - 1$ degrees of freedom (p is the number of classes).

A significant overall Q_w statistic indicated inhomogeneity (variability) among studies effect sizes and suggests existence of moderators. For comparisons between groups in a moderator analysis, Q_b estimated variance with p−1 degrees of freedom, where p is the number of classes or subgroups within a moderator. A significant Q_b statistic was taken as an indicator that the moderator explains the variance in effect sizes.

Results

Regional iron content estimated *in vivo* by various MRI techniques positively correlated with age within all ROIs: for all regions, the 95% CI did not include zero (Figures 1–5). Comparing across regions, the age-related differences in iron content were smaller in the GP (d = 0.61, 95% CI: 0.50–0.72) than in the Pt (d = 0.88, 95% CI: 0.77/0.98). The magnitude of age differences in Cd iron content (d = 0.74, 95% CI: 0.64–0.84) was intermediate between those in the Pt and the GP, and did not differ significantly from either region, although the respective 95% CI overlapped by no more than 0.08 d (standard deviation units). The magnitude of age differences in the RN (d = 0.78, 95% CI: 0.59–0.97) and SN (d = 0.71, 95% CI: 0.55–0.86) iron content also did not differ from the effects observed in other ROIs. The effect sizes were heterogeneous for all the ROIs: the Cd ($Q_w \chi^2$ (16, N = 966) = 166.68, $p < 0.05$), GP ($Q_w \chi^2$ (13, N = 782) = 93.68, $p < 0.05$), Pt ($Q_w \chi^2$ (15, N = 917) = 160.15, $p < 0.05$), RN ($Q_w \chi^2$ (4, N = 299) = 27.15, $p < 0.05$), and SN ($Q_w \chi^2$ (7, N = 396) = 31.21, $p < 0.05$). We explored potential sources of this heterogeneity.

3.1 Methodological Features as Moderators of the Effect Size

Studies included in this meta-analysis differed on multiple features. Because of a limited number of studies, we could not explore most potential moderators. However, we were able to examine two important moderators of age differences in estimated iron content: the estimation method and the treatment of age in the study (i.e., extreme age groups or a continuous age distribution).

Differences in MRI methods of iron content estimation explained a significant share of inter-study variability in age effects (Tables 2–6). Only for the Cd, all methods found equivalent age differences. In the GP, studies that used R2 calculations to estimate brain iron content produced age differences that were smaller than those noted in R2*-based measures (d = 0.29, 95% CI: 0.01–0.56 vs. d = 0.79, 95% CI: 0.58–1.00), although neither method differed from FDRI or phase (Table 3). R2-based measures in the RN (d = 0.05, 95% CI: −0.41/0.51) and SN (d = 0.16, 95% CI: −0.20/0.53) yielded no significant age differences, whereas the other methods revealed a positive association between age and iron content in both regions (Tables 5–6). Age differences in the Pt found in R2-based studies were comparable to the effects observed in R2*- and FDRI-based investigations (Table 4). However, phase measures revealed a larger age effect than any other method (d =1.94, 95% CI: 1.68–2.19).

With exception of the Pt, the R2 method systematically revealed smaller age differences in iron content across all regions relative to the other methods ($Q_w \chi^2$ = 0.81–3.61, *ns*). In comparison, age differences in FDRI estimates of iron content in the GP, RN and SN were similar to the effects yielded by other methods and equivalent across studies: $Q_w \chi^2$ (5, N = 258) = 8.44, *ns* for the GP, $Q_w \chi^2$ (1, N = 46) = 0.00, *ns* for the RN, and $Q_w \chi^2$ (2, N = 60) = 0.12, *ns* for the SN. Significant between-study heterogeneity of age effects was observed for the Cd and Pt: $Q_w \chi^2$ (5, N = 258) = 29.27, $p < 0.05$ for the Cd and $Q_w \chi^2$ (5, N = 258) = 49.79, $p < 0.05$ for the Pt. Age differences in R2* and phase measures were also heterogeneous across studies in all ROIs ($Q_w \chi^2$ = 14.07–66.88, $p < 0.05$), except for phase-based estimates in the Pt ($Q_w \chi^2$ (1, N = 178) = 1.07, *ns*). Because of a small number of studies, it was impossible to explore the reason for the observed effect heterogeneity by region.

3.1.2—*Design type (extreme age groups vs. age-continuous)* did not moderate age differences in iron concentration in the basal ganglia as there were no significant heterogeneity of effects: $Q_b \chi^2$ = 0.03–0.37, *ns*. Although extreme-group designs yielded somewhat smaller effects in these regions, the difference was not significant. However, extreme-group studies reported significantly smaller age differences in the RN and SN in comparison to the age-continuous samples (Tables 5 and 6).

Discussion

In the meta-analysis of 20 studies, we documented a robust positive correlation between age and iron content estimated from MRI in the basal ganglia, RN and SN. The greatest age-related differences were observed in the Pt, and the smallest in the GP. The smaller age effect observed in the GP may reflect the earlier onset of free iron accumulation and, as a consequence, a relatively high pallidal content in early adulthood (Aquino et al., 2009). Reaching its peak level early, GP iron content would not change substantially during the rest of the lifespan in healthy adults. Exceeding this normative asymptote, the accumulation of large amounts of iron in the GP may be a marker of neurodegenerative disease (i.e., Hallervorden and Spatz, 1922), which was intentionally excluded in the studies entered into the meta-analysis.

The mechanisms of the age-related increase in iron content are unclear. Iron is a co-factor in the production of ATP (Todorich et al., 2009) and according to some interpretations, its accumulation may, at least initially, represent an organism's attempt to meet metabolic and energetic demands needed to maintain normal function of a declining system (Bartzokis, 2011; Harder et al., 2008; Mills et al., 2011). According to this scenario, iron concentration eventually exceeds the requirements to maintain homeostasis and overwhelms cellular metabolism, thus contributing to neurodegenerative processes. Indeed, brain iron plays an important role in myelination and re-myelination throughout the lifespan (Todorich et al., 2009; Bartzokis, 2011). Yet, induced iron overload causes axonal injury and accelerated apoptosis (Zhang et al., 2009), as expected to occur in regions commonly affected by age and neurodegenerative disease (Moos et al., 2007; see Zecca et al., 2004 and Moos et al., 2004 for reviews). Even in subcortical nuclei and regions with little myelination, such as the basal ganglia and the hippocampus, larger iron content is associated with smaller volumes in healthy adults (Peran et al., 2009; Rodrigue et al., 2011). Thus, non-heme iron may be essential to maintain brain integrity, but its excessive accumulation may cause demyelination and volumetric shrinkage - the hallmarks of brain aging. In conjunction with the extant evidence, the strong positive correlation between age and iron content identified in this meta-analysis supports a general model of brain aging that is associated with oxidative stress (Harman, 1956). Future studies with direct quantification of oxidative stress and assessment of brain iron may clarify this connection.

The present conclusions are constrained by common limitations of *in vivo* methods. On MR images, myelin appears to be the main source of white-gray matter contrast (Fukunaga et al., 2010; Langkammer et al., 2012; Lodygensky et al., 2012). Although the structures examined in this review are primarily composed of neurons and their unmyelinated processes, it is important to take into account that small myelinated fibers are found in the striatum (Xiang et al., 2005) and can contribute to MRI findings that are interpreted as evidence of iron. Indeed, this may account for the notable heterogeneity in the age differences measured by R2* and FDRI in the Cd and Pt. Diffusion tensor imaging may be a useful though imperfect way to gauge the effect of myelin integrity on these measures. However, the observed age differences in fractional anisotropy of the basal ganglia are in the direction opposite to the expected (Pfefferbaum et al., 2010), and it is unclear if this finding reflects a methodological limitation or a meaningful physiological phenomenon. Further, *in vivo* methods may be biased by age-related differences in cerebral blood volume and flow (Gomori and Grossman, 1993; Schenck, 1995; Schenker et al., 1993). R2 relaxation rate decreases with age in relation to physiological changes in blood oxygenation (Wagner et al., 2012) and vascular health (Rodrigue et al., 2011), which may explain the systematic underestimation of age differences with the R2 method. Although the formulae for R2* and FDRI share the R2 relaxation term, reported age differences were equivalent and therefore these methods may be more robust than the others. The findings from R2- and R2*-based studies may be further confounded by comorbid calcification that affects these indices in the same manner as iron does and can be separated only with phase estimates of iron (Naderi et al., 1993; Haacke et al., 2005). However, the magnitude of calcium deposits and ensuing MRI effects in healthy aging is probably small.

Although the examined techniques can identify relative iron content in the brain, they allow for little specificity in conclusions about non-heme iron. The amount of iron in a given voxel is proportional to signal loss due to the magnetic influence of iron neighboring spins (R2 and FDRI), local field inhomogeneity (R2*), or phase differences (phase). In a healthy brain, the local iron deposits are sufficiently large to affect the MR signal. However, the magnitude and direction of this effect is not specific to non-heme iron, and may also reflect the influence of heme iron in circulating blood or hemosiderin. However, this possibility is unlikely as a recent study of older adults revealed little influence of the microbleeds on the estimates of brain iron content (Penke et al., 2012).

Based upon the respective underlying physical principles, each of the reviewed methods lays different claims of sensitivity and specificity of its estimates of iron content. FDRI is considered to be a more precise measure of ferritin-bound iron and less vulnerable to concomitant pathology factors (Bartzokis et al., 1994), unlike R2 and R2* (Langkammer et al., 2012), whereas phase measures are theoretically better to detect small differences in iron concentrations and distinguish iron deposits from calcification (Haacke et al., 2005). However, the present meta-analysis found that FDRI, R2* and phase studies measured equivalent age differences in iron content in all regions, except for the Pt. Even though phase measures identified a stronger age-iron association in the Pt than FDRI or R2* did, all three techniques distinguished the Pt as having the largest relative age difference among the examined regions. Therefore, in the study of healthy age differences, R2* and phase are empirically equivalent to FDRI. In practical consideration, R2* and phase methods have the benefit of using a single acquisition in one imaging system, rather than relying on two systems as is necessary for FDRI calculations.

Regardless of the method, however, *in vivo* measures underestimate iron content by averaging differences within a single voxel, in which small amounts are counted as zero. Age differences in regional iron content might have been further reduced by the stringent inclusion criteria used in this meta-analysis to avoid a bias from major neurological

pathology. The reviewed studies used an ROI approach, which emphasizes *a priori* hypothesis testing and can manually exclude vasculature (i.e., a source of heme iron) from measurements. This approach, however limits the number of anatomical regions that can be evaluated. In contrast, voxel-based approaches (see Radua and Mataix-Cols, 2012 for a review) cover the whole brain. However, too few voxel-based studies of age differences in R2* have been conducted thus far and the dearth of studies precludes quantitative comparison of voxel-based methods with ROI approaches. Thus far, ROI- and voxel-based method of iron evaluation reveal a similar pattern of regional and age-related differences (Peran et al., 2007, 2009).

Despite these limitations, the meta-analysis identified a robust positive correlation between age and iron content within the nigra striatum and smaller differences in the GP, which is consistent with post-mortem studies (Thomas et al., 1993; Hallgren and Sourander, 1958). Moreover, the observed age differences might have been overestimated because few studies controlled for a major confound of age effects – concomitant vascular risk and outright vascular pathology. In cross-sectional studies, non-linearity of age-iron content associations is thought to reflect individual differences in chronic inflammation (Zecca et al., 2004) and hypertension (Rodrigue et al., 2011), as well as in iron metabolic proteins (Bartzokis et al., 2011). Age-related iron accumulation is likely to follow a non-linear trajectory (Thomas et al., 1993; Hallgren and Sourander, 1958), although in the absence of longitudinal studies the true life-course of this phenomenon is unknown. Although a cross-sectional design may provide clues to the mean age trends, in the absence of longitudinal studies, there is little to be said about the true trajectories of age-related change and, more importantly, individual differences therein and potential mediators of change (Maxwell and Cole, 2007; Raz and Lindenberger, 2010).

4.1 Conclusions

In conclusion, presuming the validity of MRI-based estimates, advanced age is associated with higher iron content in the striatum, substantia nigra, and the red nucleus. Although MRI methods cannot readily distinguish between heme and non-heme iron, imaging studies with concurrent post-mortem assays indicate that ferritin-bound non-heme iron is the primary source of signal inhomogeneity in these subcortical nuclei (Thomas et al., 1993; see Haacke et al., 2005 for a review). Longitudinal studies with multiple imaging modalities are necessary to determine the trajectories of age-related change in regional brain iron content, individual variability therein, temporal relations among various indicators of brain integrity, and their cognitive, behavioral and health-related correlates.

Acknowledgments

Supported by the National Institutes of Health grants R37 AG-011230 to NR and training grant T32 HS-013819 to the Institute of Gerontology, Wayne State University.

References

* indicates study was included in the meta-analysis

*. Agartz I, Saaf J, Wahlund L-O, Wetterberg L. T1 and T2 relaxation time estimates in the normal human brain. Radiol. 1991; 181(2):537–543.

Anderson CM, Kaufman MJ, Lowen SB, Rohan M, Renshaw PF, Teicher MH. Brain T2 relaxation times correlate with regional cerebral blood volume. MGMA. 2005; 181:3–6.

*. Antonini A, Leenders KL, Meier D, Oertel MD, Boesiger P, Anliker M. T_2 relaxation time in patients with Parkinson's disease. Neurol. 1993; 43:697–700.

*. Aquino D, Bizzi A, Grisoli M, Garavaglia B, et al. Age-related iron deposition in the basal ganglia: quantitative analysis in healthy subjects. Radiol. 2009; 252(1):165–172.

Bartzokis G. Alzheimer's disease as homeostatic responses to age-related myelin breakdown. Neurobiol Aging. 2011; 32(8):1341–1371. [PubMed: 19775776]

*. Bartzokis G, Beckson M, Hance D, Marx P, Foster J, Marder S. MR evaluation of age-related increase of brain iron in young adult and older normal males. J Magn Reson Imaging. 1997; 15(1):29–35.

*. Bartzokis G, Cummings JL, Markham CH, Marmarelis PZ, et al. MRI evaluation of brain iron in earlier- and later-onset Parkinson's disease and normal subjects. J Magn Reson Imaging. 1999; 17(2):213–222.

*. Bartzokis G, Mintz J, Sultzer D, Marx P, Herzberg JS, Phelan CK, Marder SR. In vivo MR evaluation of age-related increases in brain iron. AJNR. 1994; 15(6):1129–1138. [PubMed: 8073983]

Bartzokis G, Sultzer D, Mintz J, Holt LE, Marx P, Phelan CK, Marder SR. In vivo evaluation of brain iron in Alzheimer's disease and normal subjects using MRI. Biol Psychiatry. 1994; 35:480–487. [PubMed: 8018799]

Bartzokis G, Lu P, Tingus K, Peters D, et al. Gender and iron genes may modify associations between brain iron and memory in healthy aging. Neuropsychopharmacology. 2011; 36:1375–1384. [PubMed: 21389980]

Bartzokis G, Lu PH, Tishler T, Peters D, et al. Prevalent iron metabolism gene variants associated with increased brain ferritin iron in healthy older men. JAD. 2010; 20:333–341. [PubMed: 20164577]

*. Bartzokis G, Tishler TA, Lu PH, et al. Brain ferritin iron may influence age- and gender-related risks of neurodegeneration. Neurobiol Aging. 2007; 28:414–423. [PubMed: 16563566]

Berg, D.; Kruger, R.; Rie, BR.; Riederer, P. Parkinson's disease. In: Youdim, M.; Riederer, P.; Mandel, S.; Battistin, L., editors. Handbook of Neurochemistry and Molecular Neurobiology: Degenerative Diseases of the Nervous System. 3. Springer; New York, NY: 2007. p. 1-20.

*. Bilgic B, Pfefferbuam A, Rohlfing T, Sullivan E, Adalsteinsson E. MRI estimates of brain iron concentration in normal aging using quantitative susceptibility mapping. NeuroImage. 2011; 59(3):2625–2635. [PubMed: 21925274]

Bizzi A, Brooks RA, Brunetti A, et al. Role of iron and ferritin in MR imaging of the brain: A study in primates at different field strengths. Radiol. 1990; 177:59–65.

Brass SD, Chen N, Mulkern R, Baksni R. Magnetic resonance imaging of iron deposition in neurological disorders. Top Magn Reson Imaging. 2006; 17(1):31–40. [PubMed: 17179895]

*. Cherubini A, Peran P, Caltagirone C, Sabatini U, Spalletta G. Aging of subcortical nuclei: Microstructural, mineralization and atrophy modifications measured in vivo using MRI. NeuroImage. 2009; 48:29–36. [PubMed: 19540925]

Drayer B. Imaging of the aging brain: Part I. normal findings. Radiol. 1988; 166:785–796.

Fisher J, Ingram D, Slagle-Webb B, Madhankumar AB, et al. Ferritin: a novel mechanism for delivery of iron to the brain and other organs. Am J Cell Physiol. 2006; 293:C641–C649.

Fukunaga M, Li TQ, van Gelderen P, de Zwart JA, Shmueli K, Yao B, Lee J, Maric D, Aronova MA, Zhang G, Leapman RD, Schenck JF, Merkle H, Duyn JH. Layer-specific variation of iron content in cerebral cortex as a source of MRI contrast. Proc Natl Acad Sci U S A. 2010; 107:3834–3839. [PubMed: 20133720]

Gomori G. Microtechnical demonstration of iron. A criticism of its methods. Am J Pathol. 1936; 12:655–663. [PubMed: 19970292]

Gomori J, Grossman R. The relation between regional brain iron and T2 shortening. AJNR. 1993; 14:1049–1050. [PubMed: 8237679]

Haacke EM, Cheng NYC, House MJ, et al. Imaging iron stores in the brain using magnetic resonance imaging. J Magn Reson Imaging. 2005; 23(1):1–25.

. Haacke EM, Miao Y, Liu M, Habib CA, Katkuri Y, Liu T, Yang Z, Lang Z, Hu J, Wu J. Correlation of putative iron content as represented by changes in R2 and phase with age in deep gray matter of healthy adults. J Magn Reson Imaging. 2010; 32:561–576. [PubMed: 20815053]

Haacke EM, Tang J, Neelavalli J, Cheng YCN. Susceptibility mapping as a means to visualize veins and quantify oxygen saturation. J Magn Reson Imaging. 2010; 32:663–676. [PubMed: 20815065]

Hallervorden J, Spatz H. Peculiar disease of the extrapyramidal system with particular affection of the globus pallidus and the substantia nigra. (Translation). Z Ges Neurol Psychiat. 1922; 79:254–302.

Hallgren B, Sourander P. The effect of age on the non-haemin iron in the human brain. J Neurochem. 1958; 3:41–51. [PubMed: 13611557]

Halliwell, B. Iron and damage to biomolecules. In: Lauffer, editor. Iron and Human Disease. CRC Press; Roca Baton, FL: 1992. p. 209-236.

Hamilton ML, Van Remmen H, Drake J, Yang H, et al. Does oxidative damage to DNA increase with age? PNAS. 2001; 98(18):10469–10474. [PubMed: 11517304]

Harder SL, Hopp KM, Ward H, Neglio H, Gitlin J, Kido D. Mineralization of the deep gray matter with age: A retrospective review with susceptibility-weighted MR imaging. AJNR. 2008; 29:176–183. [PubMed: 17989376]

Harman D. Aging: A theory based on free radical and radiation chemistry. J Gerontol. 1956; 11(3): 298–300. [PubMed: 13332224]

*. Hasan KM, Halphen C, Boska MD, Narayana PA. Diffusion tensor metrics, T_2 relaxation, and volumetry of the naturally aging human caudate nuclei in healthy young and middle-aged adults: possible implications for the neurobiology of human brain aging and disease. Magn Reson Med. 2008; 59:7–13. [PubMed: 18050345]

*. Hasan KM, Halphen C, Kamali A, Nelson FM, Wolinsky JS, Narayana PA. Caudate nuclei volume, diffusion tensor metrics, and T_2 relaxation in healthy adults and relapsing-remitting multiple sclerosis patients: Implications to understanding gray matter degeneration. J Magn Reson Imaging. 2009; 29(1):70–77. [PubMed: 19097116]

Hedges, LV.; Olkin, I. Statistical methods for meta-analysis. Academic Press; Orlando, FL: 1985.

House E, Collingwood J, Khan A, Korchazkina O, Berthon G, Exley C. Aluminum, iron, zinc and copper influence the in vitro formation of amyloid fibrils of Abeta42 in a manner which may have consequences for metal chelation therapy in Alzheimer's disease. J Alz Dis. 2004; 6(3):291–301.

Packard MG, Knowlton BJ. Learning and memory functions of the basal ganglia. Annu Rev Neurosci. 2002; 25:563–593. [PubMed: 12052921]

Jara H, Sakai O, Mankal P, Irving R, Norbash A. Multispectral quantitative magnetic resonance imaging of brain iron stores: a theoretical perspective. Top Magn Reson Imaging. 2006; 17:19–30. [PubMed: 17179894]

Johnson, BT. DSTAT 1.10: Software for the meta-analytic review of research literatures. Erlbaum; Hillsdale, NJ: 1993.

Joseph JA, Shukitt-Hale B, Casadesus G, Fisher D. Oxidative stress and inflammation in brain aging: Nutritional considerations. Neurochem Res. 2005; 30(6/7):927–935. [PubMed: 16187227]

Koeppen A. The history of iron in the brain. J Neurol Sci. 1995; 134(Suppl):1–9. [PubMed: 8847538]

*. Kruit MC, Launer LJ, Overbosch J, van Buchem MA, Ferrari MD. Iron accumulation in deep brain nuclei in migraine: a population-based magnetic resonance imaging study. Cephalalgia. 2008; 29:351–359. [PubMed: 19025553]

*. Kumar R, Delshad S, Woo MA, Macey PM, Harper RM. Age-related regional brain T2-relaxation changes in healthy adults. J Magn Reson Imaging. 2011; 35(2):300–308. [PubMed: 21987489]

Langkammer C, Krebs N, Goessler W, Scheurer E, Yen K, Fazekas F, Ropele S. Susceptibility induced gray-white matter MRI contrast in the human brain. NeuroImage. 2012; 59:1413–1419. [PubMed: 21893208]

Lauffer, R., editor. Iron and Human Disease. CRC Press; Boca Raton, FL: 1992. Introduction. Iron, aging, and human disease: Historical background and new hypotheses; p. 1-22.

Lodygensky GA, Marques JP, Maddage R, Perroud E, Sizonenko SV, Hüppi PS, Gruetter R. In vivo assessment of myelination by phase imaging at high magnetic field. NeuroImage. 2012; 59:1979–1987. [PubMed: 21985911]

Maaroufi K, Ammari M, Jeljeli M, Roy V, Sakly M, Abdelmelek H. Impairment of emotional behavior and spatial learning in adult Winstar rats by ferrous sulfate. Physiol Behav. 2009; 96:343–349. [PubMed: 19027765]

*. Martin WRW, Ye FQ, Allen PS. Increasing striatal iron content associated with normal aging. Mov Disord. 1998; 13(2):281–286. [PubMed: 9539342]

Mills E, Dong X, Wang F, Xu H. Mechanisms of brain iron transport: Insight into neurodegeneration and CNS disorders. Future Med Chem. 2010; 2(1):51–72. [PubMed: 20161623]

Moos T, Morgan EH. The metabolism of neuronal iron and its pathogenic role in neurologic disease: review. Ann N Y Acad Sci. 2004; 1012:14–26. [PubMed: 15105252]

Moos T, Rosengren Nielsen T, Skjorringe T, Morgan EH. Iron trafficking inside the brain. J Neurochem. 2007; 103(5):1730–1740. [PubMed: 17953660]

Naderi S, Colakoglu Z, Luleci G. Calcification of basal ganglia associated with pontine calcification in four cases: A radiologic and genetic study. Clin Neurol Neurosurg. 1993; 95(2):155–157. [PubMed: 8344016]

Ogg RJ, Langston JW, Haacke EM, Steen RG, Taylor JS. The correlation between phase shifts in gradient-echo MR images and regional brain iron concentration. J Magn Reson Imaging. 1999; 17(8):1141–1148.

Ordidge RJ, Gorell JM, Deniau JC, Knight RA, Helpern JA. Assessment of relative brain iron concentrations using T_2-weighted and T_2*-weighted MRI at 3 tesla. Magn Reson Med. 1994; 32:335–341. [PubMed: 7984066]

Penke L, Valdés Hernandéz MC, Maniega SM, Gow AJ, Murray C, Starr JM, Bastin ME, Deary IJ, Wardlaw JM. Brain iron deposits are associated with general cognitive ability and cognitive aging. Neurobiol Aging. 2012; 33(3):510–517.e2. Epub 2010 Jun 9. [PubMed: 20542597]

*. Peran P, Cherubini A, Luccichenti G, et al. Volume and iron content in the basal ganglia and thalamus. Hum Brain Mapp. 2009; 30:2667–2675. [PubMed: 19172651]

Peran P, Hagberg G, Luccichenti G, et al. Voxel-based analysis of R2* maps in the healthy human brain. J Magn Reson Imaging. 2007; 26:1413–1420. [PubMed: 18059009]

*. Pfefferbaum A, Adalsteinsson E, Rohfling T, Sullivan EV. MRI estimates of brain iron concentration in normal aging: Comparison of field-dependent (FDRI) and phase (SWI) methods. NeuroImage. 2009; 47(2):493–500. [PubMed: 19442747]

*. Pfefferbaum A, Adalsteinsson E, Rohlfing T, Sullivan EV. Diffusion tensor imaging of deep gray matter brain structures: Effects of age and iron concentration. Neurobiol Aging. 2010; 31(3):482–500. [PubMed: 18513834]

*. Pujol J, Junque C, Vendrell P, et al. Biological significance of iron-related magnetic resonance imaging changes in the brain. Arch Neurol. 1992; 49(7):711–717. [PubMed: 1497497]

Quintana C, Bellefqih S, Laval JY, et al. Study of the localization of iron, ferritin, and hemosedrin in Alzheimer's disease hippocampus by analytical microscopy at the subcellular level. J Struct Biol. 2006; 153:42–54. [PubMed: 16364657]

Radua J, Mataix-Cols D. Meta-analytic methods for neuroimaging data explained. Biol Mood Anxiety Disord. 2012; 2(1):6–16. [PubMed: 22737993]

Raz, N.; Kennedy, KM. A systems approach to the aging brain: Neuroanatomic changes, their modifiers, and cognitive correlates. In: Jagust, W.; D'Esposito, M., editors. Imaging the Aging Brain. Oxford University Press; 2009. p. 43-70.

Raz N, Lindenberger U. News of cognitive cure for age-related brain shrinkage is premature: a comment on Burgmans et al., (2009). Neuropsychol. 2010; 24(2):255–257.

Rival T, Page RM, Chandraratna DS, et al. Fenton chemistry and oxidative stress mediate the toxicity of the *B*-amyloid peptide in a *Drosophila* model of Alzheimer's disease. Eur J Neurosci. 2009; 29:1335–1347. [PubMed: 19519625]

*. Rodrigue KM, Haacke EM, Raz N. Differential effects of age and history of hypertension of regional brain volumes and iron. NeuroImage. 2011; 54:750–759. [PubMed: 20923707]

Rodrigue KM, Daugherty AM, Haacke EM, Raz N. The role of hippocampal iron concentration and hippocampal volume in age-related differences in memory performance. Cereb Cortex. 2012 Epub 2012 May 29.

Schenck J. Imaging of brain iron by magnetic resonance: T2 relaxation at different field strengths. J Neurol Sci. 1995; 134(Suppl):10–18. [PubMed: 8847539]

Schenker C, Meier D, Wichmann W, Boesiger P, Valavanis A. Age distribution and iron dependency of the T2 relaxation time in the globus pallidus and putamen. Neuroradiol. 1993; 35:119–124.

Siemonsen S, Finsterbusch J, Matschke J, Loernzen A, Ding X-Q, Fiehler J. Age-dependent normal values of T2* and T2′ in brain parenchyma. Am J Neuroradiol. 2008; 29:950–955. [PubMed: 18272561]

Singh A, Isaac AO, Luo X, Mohan ML, Cohen ML, Chen F, Kong Q, Bartz J, Singh N. Abnormal brain iron homeostasis in human and animal prion disorders. PLoS Pathog. 2009; 5:e1000336. [PubMed: 19283067]

Spatz H. On the visualization of iron in the brain, especially in the centers of the extrapyramidal motor system. Z ges Neurol Psychiat. 1922; 77:261–390.Koeppen A. 1992

Thomas LO, Boyoko OB, Anthony DC, Burger PC. MR detection of brain iron. Am J Neuroradiol. 1993; 14(5):1043–1048. [PubMed: 8237678]

Tingey AH. The iron content of the human brain –II. J Ment Sci. 1938; 84:980–984.

Todorich B, Pasquini JM, Garcia CI, Paez PM, Connor JR. Oligodendrocytes and myelination: The role of iron. Glia. 2009; 57:467–478. [PubMed: 18837051]

Vymazal J, Brooks RA, Patronas N, Hajek M, Bulte JWM, Di Chiro G. Magnetic resonance imaging of brain iron in health and disease. J Neurol Sci. 1995a; 134(Suppl):19–26. [PubMed: 8847541]

Vymazal J, Hajek M, Patronas N, Fiedd JN, Butte JWM, Baurngarner C, Tran V, Brooks RA. The quantitative relation between T1-weighted and T2-weighted MRI of normal gray matter and iron concentration. J Magn Reson Imaging. 1995b; 5(5):554–560. [PubMed: 8574041]

Wagner M, Jurcoane A, Volz S, Magerkurth J, Zanella FE, Neumann-Haefelin T, Deichmann R, Singer OC, Hattingen E. Age-related changes of cerebral autoregulation: New insights with quantitative T2′-mapping and pulsed arterial spin-labeling MR imaging. AJNR. 2012 Epub 2012 Jun 14.

Xiang Z, Nesterov EE, Skoch J, Lin T, Hyman BT, Swager TM, Bacskai BJ, Reeves SA. Detection of myelination using a novel histological probe. J Histochem Cytochem. 2005; 53:1511–1516. [PubMed: 16046669]

*. Xu X, Wang Q, Zhang M. Age, gender, and hemispheric differences in iron deposition in the human brain : An *in vivo* MRI study. NeuroImage. 2008; 40:35–42. [PubMed: 18180169]

Yamada K, Gonzalez G, Oztergaard L, Komili S, et al. Iron-induced susceptibility effect at the globus pallidus causes underestimation of flow and volume on dynamic susceptibility contrast-enhanced MR perfusion images. Am J Neuroradiol. 2002; 23:1022–1029. [PubMed: 12063236]

Zecca L, Stroppolo A, Gatti A, Tampellini D, Toscani M, Gallorini M, Glaveri G, Aroslo P, Santambroglo P, Farlello RG, Katatekin E, Klenlnman MH, Turro N, Hornyklewicz O, Zucca FA. The role of iron and copper molecules in the neuronal vulnerability of locus coeruleus and substantia nigra during aging. PNAS. 2004; 101(26):9843–9848. [PubMed: 15210960]

Zhang S, Wang J, Song N, Xie J, Jiang H. Up-regulation of divalent metal transporter 1 is involved in 1-methyl-4-phenylpyridinium (MPP+)-induced apoptosis in MES23.5 cells. Neurobiol Aging. 2009; 30:1466–1476. [PubMed: 18191877]

Highlights

- MRI studies inconsistently report higher brain iron content in older adults.
- This meta-analysis found high iron content with advanced age in several regions.
- Age-related iron content was higher in the neostriatum and substantia nigra.
- Differences in estimation method partly explained the variability between studies.

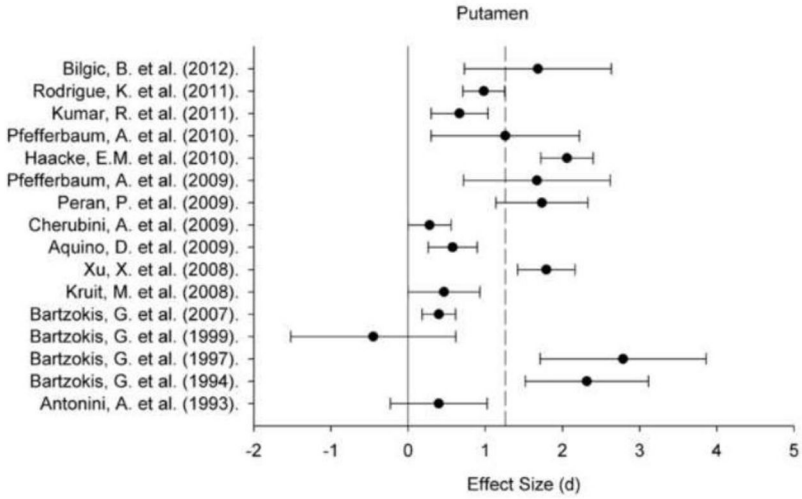

Figure 1.

A plot of effect sizes for age differences in iron content of the putament (Pt). Sample size-corrected effect sizes (*d*) are shown with 95% confidence intervals and the median value across studies is marked with the dotted line. Confidence intervals not including zero indicates significant age-related difference.

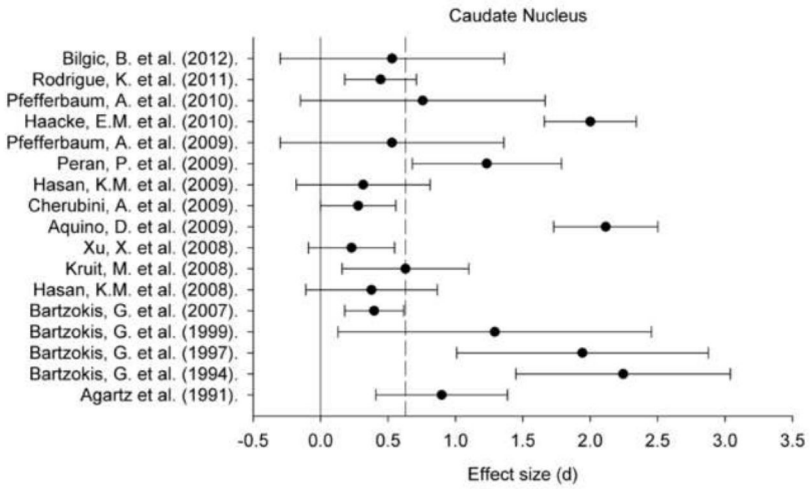

Figure 2.

A plot of effect sizes for age differences in iron content of the caudate nucleus (Cd). Sample size-corrected effect sizes (*d*) are shown with 95% confidence intervals and the median value across studies is marked with the dotted line. Confidence intervals not including zero indicates significant age-related difference.

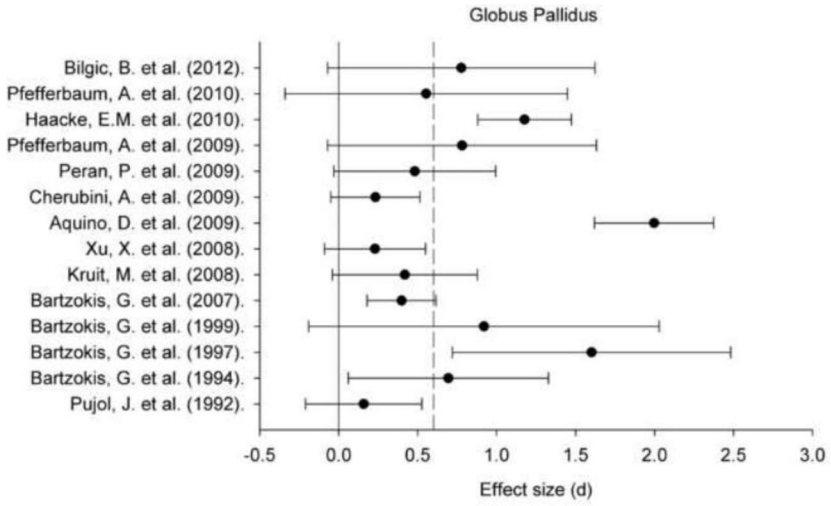

Figure 3.

A plot of effect sizes for age differences in iron content of the globus pallidus (GP). Sample size-corrected effect sizes (*d*) are shown with 95% confidence intervals and the median value across studies is marked with the dotted line. Confidence intervals not including zero indicates significant age-related difference.

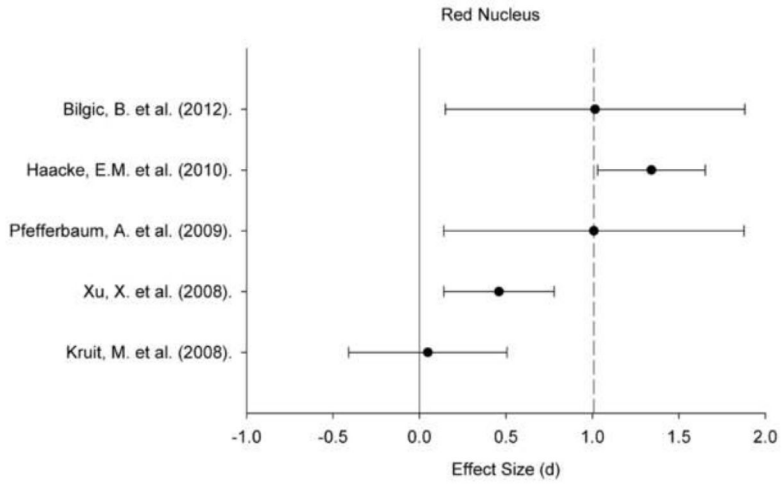

Figure 4.

A plot of effect sizes for age differences in iron content of the red nucleus (RN). Sample size-corrected effect sizes (*d*) are shown with 95% confidence intervals and the median value across studies is marked with the dotted line. Confidence intervals not including zero indicates significant age-related difference.

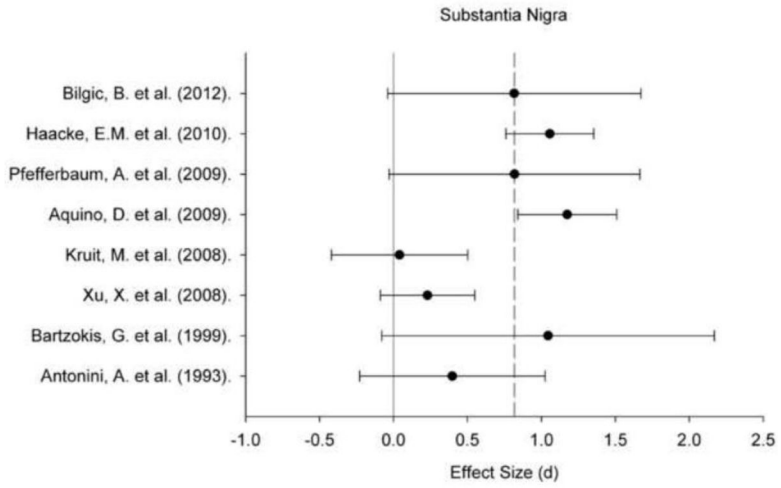

Figure 5.

A plot of effect sizes for age differences in iron content of the substantia nigra (SN). Sample size-corrected effect sizes (*d*) are shown with 95% confidence intervals and the median value across studies is marked with the dotted line. Confidence intervals not including zero indicates significant age-related difference.

Table 1

List of studies with respective effect sizes (r) per region of interest.

	Effect Size *r*									
Study	**Cd**	**GP**	**Pt**	**RN**	**SN**	**N (Y/O)**	**Age Range (mean)**	**Magnetic Field**	**Method**	**Design**
Agartz et al. (1991).	0.42					64	19–84 (55.0)	0.02	R2	Continuous
Antonini, A. et al. (1993).	---	---	0.20		0.20	20	40–68 (52.1)	1.5	R2	Continuous
Aquino, D. et al. (2009).	0.73	0.71	0.28		0.51	63	20–80	1.5	R2*	Continuous
Bartzokis, G. et al. (1994).	0.76	0.34	0.77			20	20–81 (55.5)	.5/1.5	FDRI	Continuous
Bartzokis, G. et al. (1997).	0.72	0.65	0.83			13	21–77 (38.5)	.5/1.5	FDRI	Continuous
Bartzokis, G. et al. (1999).	0.57	0.44	−0.23		0.49	6/8	56–75	.5/1.5	FDRI	Group
Bartzokis, G. et al. (2007).	0.2	0.2	0.2			165	19–82 (53.2)	.5/1.5	FDRI	Continuous
Bilgic, B. et al. (2012)	0.27	0.37	0.66	0.47	0.39	11/12	21–86 (49.2)	1.5/3.0	FDRI	Group
Cherubini, A. et al. (2009).	0.14	0.12	0.14			100	20–70 (41.0)	3.0	R2*	Continuous
Haacke, E.M. et al. (2010).	0.71	0.51	0.72	0.56	0.47	100	20–69 (43.0)	1.5	Phase	Continuous
Hasan, K.M. et al. (2008).	0.19					33	19–59 (36.9)	3.0	R2	Continuous
Hasan, K.M. et al. (2009).	0.16					32	22–59 (38.7)	3.0	R2	Continuous
Kruit, M. et al. (2008).	0.3	0.21	0.23	0.02	0.02	43/32	30–60	1.5	R2	Group
Kumar, R. et al. (2011).			0.32			60	31–66	3.0	R2	Continuous
Peran, P. et al. (2009).	0.54	0.24	0.67			30	20–41 (29.3)	3.0	R2*	Continuous
Pfefferbaum, A. et al. (2009).	0.27	0.38	0.65	0.46	0.39	11/12	21–86 (49.2)	1.5/3.0	FDRI	Group
Pfefferbaum, A. et al. (2010).	0.37	0.28	0.55			10/10	22–79 (50.4)	3.0	R2	Group
Pujol, J. et al. (1992).		0.08				58	41–76	1.5	R2	Continuous
Rodrigue, K. et al. (2011).	0.22		0.44			113	(53.96)	1.5	R2*	Continuous
Xu, X. et al. (2008).	0.12	0.12	0.67	0.23	0.12	78	22–78 (43.3)	1.5	Phase	Continuous

Note: Cd = caudate; GP = globus pallidus; Pt = putamen; RN = red nucleus; SN = substantia nigra;. Y = young; O = old for group comparison studies; r – Pearson correlation between age and the estimate of iron content; --- indicates an effect was reported but not included in the meta-analysis due to insufficient data.

Table 2

Overall categorical and moderator analysis within the caudate.

						Homogeneity Tests	
Moderator	***k***	***N***	**Mean weighted effect size (*d*)**	**95% CI for *d***		**Mean Weighted *r***	**$(Q_b)^a$**	**$(Q_w)^b$**
Overall	17	966	0.74	0.64	0.84	0.35		166.68 *
Method							10.72 *	
R2 *	4	306	0.76	0.59	0.92	0.35		66.88 *
R2	5	224	0.57	0.34	0.81	0.28		3.61
FDRI	6	258	0.46	0.26	0.66	0.22		29.27 *
Phase	2	178	0.56	0.35	0.77	0.27		56.21 *
Design							0.19	
Grouped	5	155	0.67	0.34	0.99	0.32		1.38
Continuous	12	811	0.74	0.64	0.85	0.35		165.10 *

Note: All effect sizes are significant, as 95% confidence intervals (CI) do not include zero. ‘k’ is the number of effect sizes included in the analysis, and N represents the cumulative sample size across studies.

* indicates significance at $p < 0.05$.

a effect size differs by moderator.

b heterogeneity across studies within moderator class.

Table 3

Overall categorical and moderator analysis within the globus pallidus.

						Homogeneity Tests	
Moderator	***k***	***N***	**Mean weighted effect size (*d*)**	**95% CI for *d***	**Mean Weighted (r)**	**$(Q_b)^a$**	**$(Q_w)^b$**
Overall	14	782	0.61	0.50 0.72	0.29		93.68 *
Method						10.18 *	
R2 *	3	193	0.79	0.58 1.00	0.37		55.73 *
R2	3	153	0.29	0.01 0.56	0.14		1.13
FDRI	6	258	0.53	0.34 0.72	0.26		8.44
Phase	2	178	0.73	0.51 0.94	0.34		18.20 *
Design						0.03	
Grouped	5	155	0.58	0.26 0.91	0.28		1.25
Continuous	9	627	0.61	0.50 0.73	0.29		92.40 *

Note: All effect sizes are significant, as 95% CI do not include zero. ‘k’ is the number of effect sizes included in the analysis, and N represents the cumulative sample size across studies.

* indicates significance at $p < 0.05$.

[a] effect size differs by moderator.

[b] heterogeneity across studies within moderator class.

Table 4

Overall categorical and moderator analysis within the putamen.

						Homogeneity Tests	
Moderator	***k***	***N***	**Mean weighted effect size (*d*)**	**95% CI for *d***		**Mean Weighted (*r*)**	**(Q_b)[a]**	**(Q_w)[b]**
Overall	16	917	0.88	0.77	0.98	0.40		160.15 *
Method							81.61 *	
R2 *	4	306	0.70	0.54	0.86	0.33		25.01 *
R2	4	175	0.60	0.35	0.86	0.29		2.67
FDRI	6	258	0.67	0.47	0.86	0.32		49.79 *
Phase	2	178	1.94	1.68	2.19	0.70		1.07
Design							0.37	
Grouped	5	155	0.78	0.44	1.11	0.36		14.63 *
Continuous	11	762	0.89	0.78	0.99	0.41		145.16 *

Note: All effect sizes are significant, as 95% CI do not include zero. 'k' is the number of effect sizes included in the analysis, and N represents the cumulative sample size across studies.

* indicates significance at $p < 0.05$.

[a] effect size differs by moderator.

[b] heterogeneity across studies within moderator class.

Table 5

Overall categorical and moderator analysis within the red nucleus.

						Homogeneity Tests	
Moderator	***k***	***N***	**Mean weighted effect size (*d*)**	**95% CI for *d***	**Mean Weighted (*r*)**	**$(Q_b)^a$**	**$(Q_w)^b$**
Overall	5	299	0.78	0.59 0.97	0.36		27.15 *
Method						11.83 *	
R2	1	75	0.05	−0.41 0.51	0.02		---
FDRI	2	46	1.01	0.40 1.62	0.45		0.00
Phase	2	178	0.92	0.70 1.14	0.42		15.31 *
Design						5.75 *	
Grouped	3	121	0.39	0.03 0.76	0.19		6.08
Continuous	2	178	0.92	0.70 1.14	0.42		15.31 *

Note: Significant effect sizes are indicated by 95% CI that do not include zero. ‘k’ is the number of effect sizes included in the analysis, and N represents the cumulative sample size across studies.

* indicates significance at $p < 0.05$.

^{a} effect size differs by moderator.

^{b} heterogeneity across studies within moderator class.

Table 6

Overall categorical and moderator analysis within the substantia nigra.

						Homogeneity Tests	
Moderator	***k***	***N***	**Mean weighted effect size (*d*)**	**95% CI for *d***	**Mean Weighted (*r*)**	**$(Q_b)^a$**	**$(Q_w)^b$**
Overall	8	396	0.71	0.55 0.86	0.33		31.21 *
Method						16.20 *	
R2 *	1	63	1.17	0.84 1.51	0.51		
R2	2	95	0.16	−0.20 0.53	0.08		0.81
FDRI	3	60	0.87	0.34 1.40	0.40		0.12
Phase	2	178	0.67	0.45 0.88	0.32		14.07 *
Design						3.91 *	
Grouped	4	135	0.39	0.05 0.74	0.19		5.47
Continuous	4	261	0.78	0.61 0.96	0.37		21.83 *

Note: Significant effect sizes are indicated by 95% CI do not include zero. ‘k’ is the number of effect sizes included in the analysis, and N represents the cumulative sample size across studies.

* indicates significance at $p < 0.05$.

[a] effect size differs by moderator.

[b] heterogeneity across studies within moderator class.